Effects of triaxiality and residual np interaction in the proton emission from ^{140}Ho

Pooja Siwach,[1] P. Arumugam,[2,*] S. Modi,[3] L. S. Ferreira,[4] and E. Maglione[4]
[1]*Department of Physics, University of Wisconsin–Madison, Madison, Wisconsin 53706, USA*
[2]*Centre for Photonics and Quantum Communication Technology, and Department of Physics, Indian Institute of Technology Roorkee, Roorkee 247667, Uttarakhand, India*
[3]*Department of Physics, BIT Sindri, Dhanbad, Jharkhand 828121, India*
[4]*Centro de Física e Engenharia de Materiais Avançados CeFEMA, and Instituto Superior Técnico, Universidade de Lisboa, Avenida Rovisco Pais, P1049-001 Lisbon, Portugal*

(Received 27 March 2022; accepted 23 September 2022; published 20 October 2022)

We present a detailed theoretical investigation of proton emission from ^{140}Ho within the nonadiabatic quasiparticle approach. The calculated proton emission half-life reproduces well the measured data. The importance of triaxiality and of the residual np interaction are studied. The ground state spin and parity of ^{139}Dy (daughter) and ^{140}Ho (parent) are ascertained unambiguously as $7/2^+$ and 3^-, respectively, by analyzing the rotational energies, half-lives, and branching ratios.

DOI: 10.1103/PhysRevC.106.044322

I. INTRODUCTION

When the nuclear landscape limits are crossed on the proton-rich side, nuclei become incapable of holding more protons, resulting in spontaneous proton emission. However, due to the high Coulomb barrier in nuclei with $Z > 50$, the proton spends enough time inside the nucleus. Therefore, this phenomenon has been studied a lot both theoretically and experimentally [1], and provides a unique tool in unveiling the structural properties of nuclei at extreme limits. From the experimental perspective, if the proton emission half-life is too short, the nuclei cannot be efficiently separated and implanted in a detector. If the half-life is longer, the decay process will be superseded by β^+ decay. Challenging measurements that stretch this allowed time interval recently became feasible [2–5], for example, with the new generation facility BigRIPS [6], where it was possible to discover ^{72}Rb [2].

Proton emission from an odd-odd nucleus populates the states of an odd-A daughter nucleus. Therefore, the ground state and level scheme of the latter, which are hard to explore experimentally in this exotic region, can be identified theoretically through the interpretation of proton emission and fine structure data of odd-odd nuclei. A nucleus of special interest is ^{140}Ho, due to its location in the middle of the shell. The nuclei below ^{140}Ho display a prolate deformation, whereas for higher mass a transition region to oblate deformation begins. According to the macroscopic-microscopic calculations [7], the transition appears to be between prolate ^{144}Ho and oblate ^{145}Ho. Furthermore, the deviation from the K isomerism in this mass region [8,9] suggests a significant K mixing that can be explained only with the gamma deformation. The emitted proton carries information about both parent and daughter states. Therefore, the study of proton emission can be a perfect tool to confirm these predictions.

The first identification of proton emission in ^{140}Ho was reported in Ref. [10]. In the theoretical study [11] based on the adiabatic approach and assuming axial symmetry, the ground state was suggested to be one among 0^-, 6^-, and 8^+ states. The model used was very simple and some features were taken into account approximately. For example, the excitation of the rotor was considered with an infinite moment of inertia, the residual pairing interaction was incorporated through a spectroscopic factor only, and the residual neutron-proton interaction was ignored. Therefore, the identification of the ground state spin and parity of ^{140}Ho along with the deformation is still uncertain. The ambiguities in the identification of the ground state of the daughter nucleus ^{139}Dy further increase the complications. The neighboring proton emitting nucleus ^{141}Ho is found to be triaxial [12]. Hence, a rigorous theoretical approach incorporating the triaxial behavior and a proper treatment of the residual neutron-proton (np) interaction is required. In the present work, we intend to explore the properties of ^{140}Ho utilizing the recently developed nonadiabatic quasiparticle approach [13] to study the triaxial odd-odd nuclei.

II. THEORETICAL FRAMEWORK

In our approach, the valence proton and neutron are coupled to the triaxially deformed even-even core in a microscopic way [13]. The triaxial Woods-Saxon potential is taken as the nuclear mean field potential along with the spin-orbit and Coulomb potentials. The residual pairing interaction is dealt with using the BCS approach. The matrix elements of the rotor appear explicitly, imparting the advantage of utilizing the measured data. The residual neutron-proton (np) interac-

*Corresponding author: arumugam@ph.iitr.ac.in

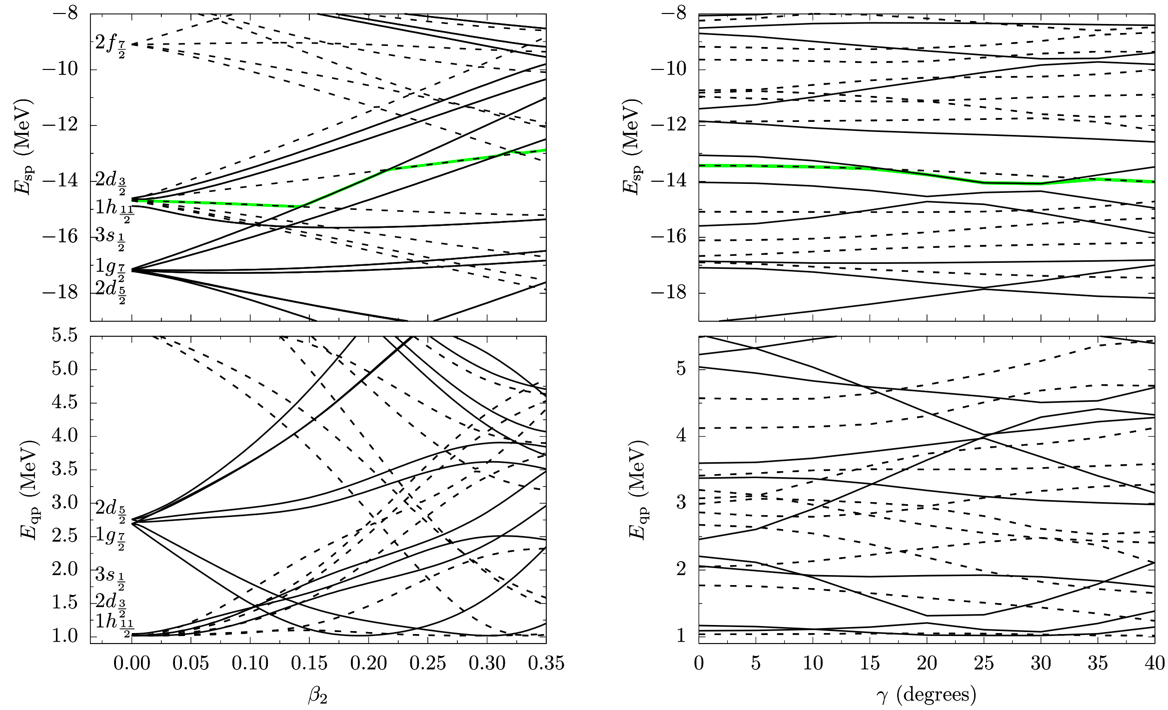

FIG. 1. Single-particle (top panels) and quasiparticle (bottom panels) levels for neutrons in ^{139}Dy as a function of $\beta_2(\beta_4 = 0.188\beta_2)$ at $\gamma = 0^\circ$ (left) and as a function of γ at $\beta_2 = 0.244$ and $\beta_4 = -0.046$ (right). The solid and dashed lines correspond to the positive and negative parity states, respectively. The green lines represent the state of the valence particles. At zero deformation, degenerate states are labeled by the quantum numbers nl_j.

tion is incorporated in two forms [13], namely, the constant potential form and zero-range interaction.

The decay width is proportional to the overlap of initial and final state wave functions. The initial state wave function, i.e., of the parent nucleus, can be expressed as [14]

$$\Psi_{IM} = \sqrt{\frac{2I+1}{16\pi^2}} \sum_{\Omega_p\Omega_n\Omega K} a^I_{\Omega_p\Omega_n\Omega K}\big[D^I_{MK}\chi^{\Omega_p\Omega_n}_{\Omega} + (-1)^{I-j_p-j_n} D^I_{M-K} R_i \chi^{\Omega_p\Omega_n}_{\bar{\Omega}}\big], \quad (1)$$

where $\chi^{\Omega_p\Omega_n}_{\Omega} = \phi_{j_p\Omega_p}\phi_{j_n\Omega_n}$ represents the product of single-particle wave functions calculated in the Woods-Saxon mean field potential. The quantities $j_{p(n)}$ and $\Omega_{p(n)}$ refer to the total angular momentum of the proton (neutron) and its projection on the 3-axis, respectively, and $\Omega = \Omega_p \pm \Omega_n$. I is the total angular momentum of the system, and K and M are its projections on the 3-axis and z axis, respectively. R_i represents the operator for rotation along the second intrinsic axis. a's are the mixing coefficients for the collective states represented by the corresponding quantum numbers. The wave function of the triaxial odd-A daughter nucleus is given by

$$\Psi_{I_dM_d} = \sqrt{\frac{2I_d+1}{16\pi^2}} \sum_{j_n\Omega_nK_d} c^{I_d}_{j_n\Omega_nK_d}\big[D^{I_d}_{M_dK_d}\phi_{j_n\Omega_n} + (-1)^{I_d-j_n} D^{I_d}_{M_d-K_d}\phi_{j_n,-\Omega_n}\big], \quad (2)$$

where the symbols have the same meaning as in the parent wave function with d denoting daughter.

From the overlap of the initial and the final state wave functions, we get the partial decay width corresponding to the emitted proton given by [14,15]

$$\Gamma^{II_d}_{l_pj_p} = \frac{\hbar^2 k}{\mu}\left(\frac{2I_d+1}{2I+1}\right)\Bigg| \sum_{j_n\Omega_n\Omega_pK_d\Omega K} c^{I_d}_{j_n\Omega_nK_d} a^I_{\Omega_p\Omega_n\Omega K} \times [\langle I_dK_d j_p\Omega_p|IK\rangle + (-1)^{I_d-K_d}\langle I_d - K_d j_p\Omega_p|IK\rangle] u_{\Omega_p} N^{\Omega_p}_{l_pj_p}\Bigg|^2, \quad (3)$$

where $N^{\Omega_p}_{l_pj_p} = \frac{\phi^{\Omega_p}_{l_pj_p}(R)}{G_{l_p}(kR)+\iota F_{l_p}(kR)}$ is the asymptotic normalization constant with F and G as the regular and irregular parts of Coulomb wave function. The quantity $\phi^{\Omega_p}_{l_pj_p}(R)$ is the radial part of the proton wave function at distance R, and k is the momentum of the proton. $u^2_{\Omega_p}$ denotes the probability of the corresponding proton level to be empty in the daughter nucleus. The quantities in the angular brackets represent the Clebsch-Gordan coefficients. The total decay width Γ^{II_d} can be obtained by summing over all the possible states, and the corresponding half-life is obtained by $T_{1/2} = \hbar \ln 2/\Gamma^{II_d}$.

III. RESULTS AND DISCUSSION

We start our investigation with the daughter nucleus ^{139}Dy to which the proton emission from ^{140}Ho proceeds. The single-particle energy levels for neutrons in ^{139}Dy are given in Fig. 1 considering axial and triaxial deformations. For the triaxial case, the quadrupole and hexadecapole deforma-

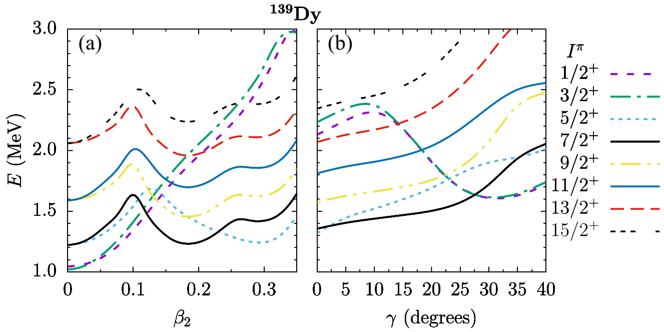

FIG. 2. Rotational energies of ^{139}Dy for positive parity states (a) with varying $\beta_2(\beta_4 = 0.188\beta_2)$ and (b) with varying γ at $\beta_2 = 0.244$ and $\beta_4 = -0.046$.

tion parameters are considered to be $\beta_2 = 0.244$ and $\beta_4 = -0.046$, respectively, following Ref. [12]. The positive parity orbitals of $d_{3/2}$, $s_{1/2}$, $g_{7/2}$, and $d_{5/2}$ parentage and negative parity orbitals of $h_{11/2}$ and $f_{7/2}$ parentage are closer to the Fermi surface. As one can notice from the quasiparticle energies in the probable deformation region, the lowest lying positive and negative parity levels are of $g_{7/2}$ and $h_{11/2}$ parentage, respectively. Increasing γ, there are many crossings mainly in the positive parity levels. For example, at $\gamma > 25^\circ$, the lower lying positive parity levels change drastically, which leads to a different configuration. In this deformation region, the lowest lying positive and negative parity levels are almost degenerate. Therefore, we investigate both possibilities for the ground state of the daughter.

To study the behavior of daughter ^{139}Dy, we consider the positive parity single-particle levels from 16th to 22nd (counted from the bottom). For the negative parity states, the single-particle levels from 14th to 21st are considered. The calculated positive and negative parity rotational states are given in Figs. 2 and 3, respectively. At zero deformation, the rotational states follow the behavior of the even-even core. With an increase in deformation, the rotational levels mimic the trend of quasiparticle energies. For example, in case of positive parity states, at $\beta_2 \lesssim 0.12$ the lowest lying states are $1/2^+$ and $3/2^+$ originating from the couplings to $3s_{1/2}$ and $2d_{3/2}$. In the deformation region $0.12 \lesssim \beta_2 \lesssim 0.24$, due to the crossings of $1g_{7/2}$ orbitals, the lowest state turns out to be $7/2^+$. We see similar features with the increase in triaxial deformation γ. In the probable axial deformation region, the lowest lying state is $5/2^+$. With the inclusion of triaxiality, in the $10^\circ \lesssim \gamma \lesssim 28^\circ$ region, the $7/2^+$ state becomes the lowest in energy. We expect a triaxial deformation $\gamma \approx 20^\circ$, as learned from the study of ^{141}Ho [12]. In case of negative parity states, the lowest lying state is $9/2^-$ throughout the probable deformation region. Given the above discussion, we investigate the possibility of proton emission to both states, i.e., $7/2^+$ and $9/2^-$ of the daughter.

It is well established that the ground state proton emission in ^{141}Ho occurs from the $7/2^-$ state [12]. Therefore, to study the rotational states and the corresponding proton emission half-lives of ^{140}Ho, we couple the negative parity levels of protons from 14th to 19th, which include orbitals of $h_{11/2}$ and $f_{7/2}$ parentage. For neutrons, we retain the levels considered in the case of ^{139}Dy. The resulting rotational states and half-lives for both the negative and positive parity states are given in Fig. 4. In the case of negative parity states, 3^- is the lowest in energy for $\gamma \lesssim 25^\circ$. The half-life is also closer to the experimental one. We observed from our analysis (not presented here) that with a slight increase in β_2 the half-life for 3^- comes closer to the measured one without changing the conclusions for the other states. At γ close to 25°, the 4^-, 5^-, and 6^- states are almost degenerate with 3^-. Also, the half-lives for these states are in the agreement with the experimental data. As we will see soon, the residual *np* interaction can be helpful in eradicating these ambiguities. At $\gamma \approx 35^\circ$, the half-life corresponding to the 5^- state is in very nice agreement with the experimental one, and it is the lowest in energy. However, the $7/2^+$ state of the daughter nucleus is not the lowest one at such a large γ. Also, from previous studies of ^{141}Ho, the γ is expected to be nearly 20°. In case of positive parity states, in the probable γ region, the 8^+ state is the lowest in energy and is almost degenerate with 3^+. The proton emission half-life corresponding to the 8^+ state does not agree with the measured data. At $\gamma \gtrsim 25^\circ$, the half-lives corresponding to states from 3^+ to 7^+ agree with the measured data. The branching ratios can be utilized to further eradicate these ambiguities, and are explained later.

We investigate the role of residual *np* interaction, incorporating it in two forms, namely, the constant potential form and the zero-range interaction [13]. Since data are scarce in this exotic region, we study their role only qualitatively, with chosen standard values for the strength parameters V, V_N, α, and W. The results with the constant potential form in the case of negative parity states are given in Fig. 5. We consider three combinations of strength parameters V_{GM} and V_N. For all these combinations, the 3^- state is the lowest in energy in the probable deformation region. Hence, it resolves the ambiguities observed in the absence of residual *np* interaction where several states are close to 3^- at $\gamma \lesssim 25^\circ$ and are almost degenerate at $\gamma \approx 25^\circ$ The energy splitting due to V_N is more than the one due to V_{GM}, indicating a stronger Newby shift for the 3^- state. It can be observed that the half-lives are almost insensitive to Newby shift, except at $\gamma = 0^\circ$. Similarly, when we introduce Gallagher-Moszkowski (GM) splitting, the trend in resulting half-lives is almost the same as that observed in the absence of *np* interaction but with an upward shift. This

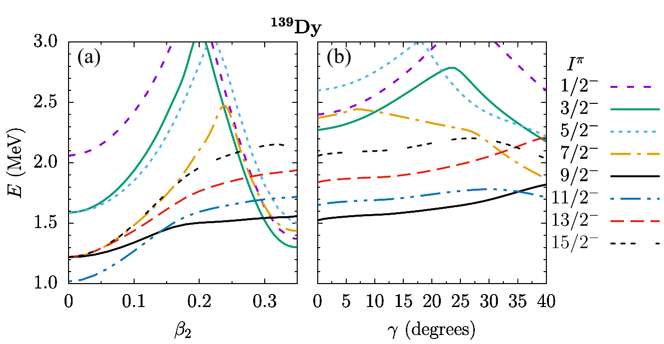

FIG. 3. Same as Fig. 2 but for negative parity states.

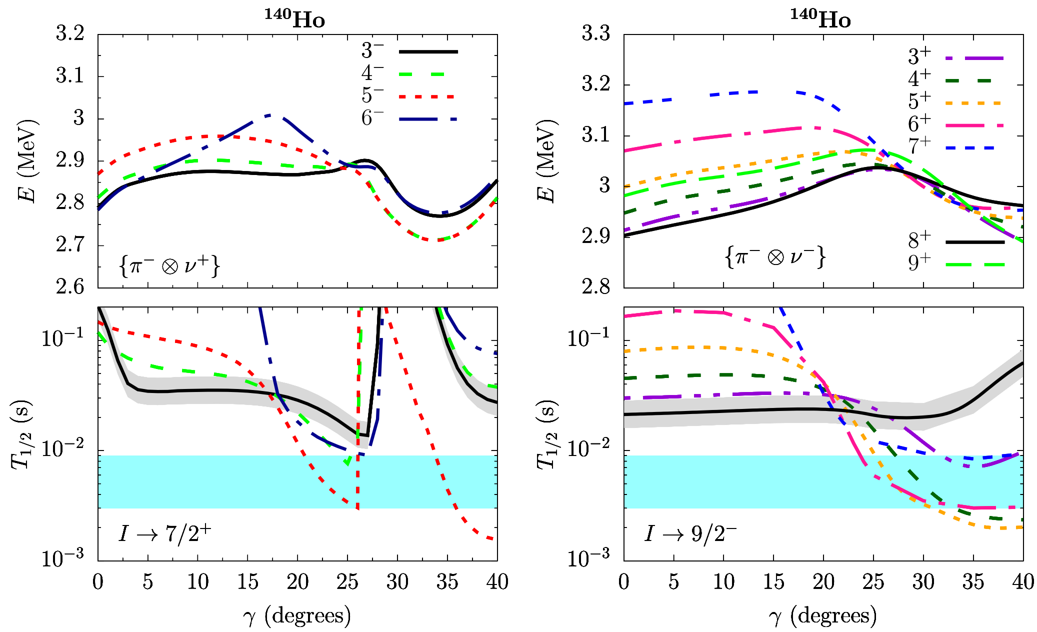

FIG. 4. Rotational energies (top panels) and the proton emission half-lives (bottom panels) from negative parity states of ^{140}Ho to the $7/2^+$ (left) state of the daughter and from positive parity states of ^{140}Ho to the $9/2^-$ (right) state of the daughter. The shaded area in the calculated half-life represents the possible error due to uncertainty in the measured Q_p value. The cyan region corresponds to the experimental half-life of proton emission [10].

behavior can be understood in terms of the contribution of single-particle configurations.

The results obtained with the zero-range interaction are given in Fig. 6. The lowest lying state is 3^- for both sets of parameters. Similarly to the case of constant potential form, there is an upward shift in the corresponding half-lives. As stated earlier, in this qualitative analysis, no attempt has been made to obtain a better fit for half-lives by tuning the parameters of *np* interaction. However, it is important to study the role of *np* interaction on rotational energies

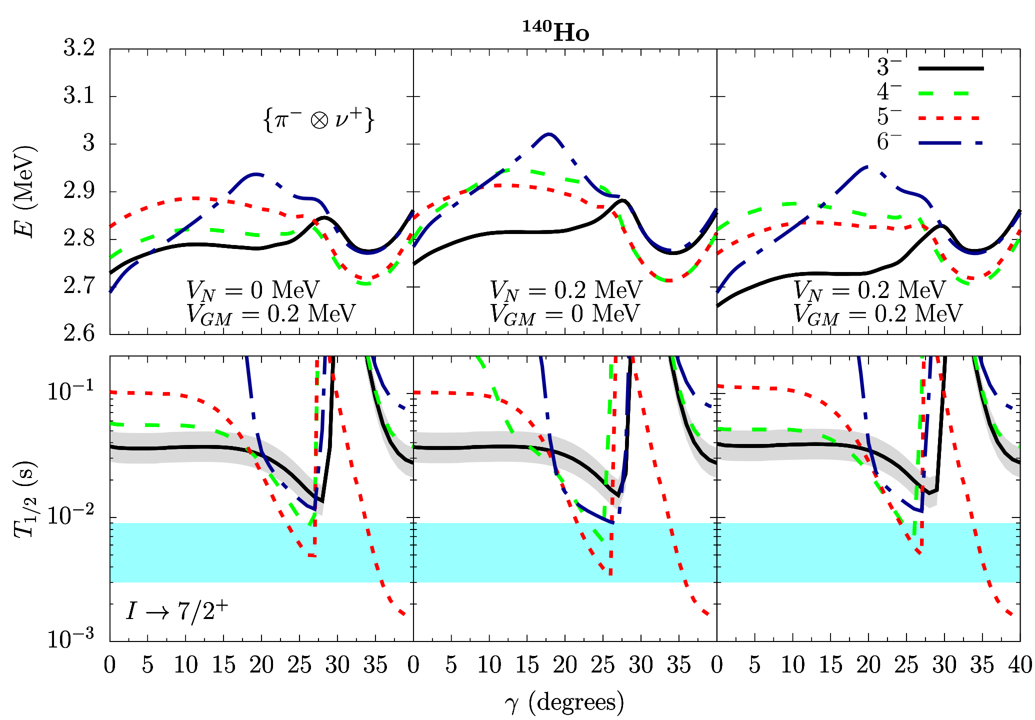

FIG. 5. Rotational energies (top panels) and the proton emission half-lives (bottom panels) from negative parity states of ^{140}Ho to the $7/2^+$ state of the daughter for different sets of parameters of constant potential *np* interaction.

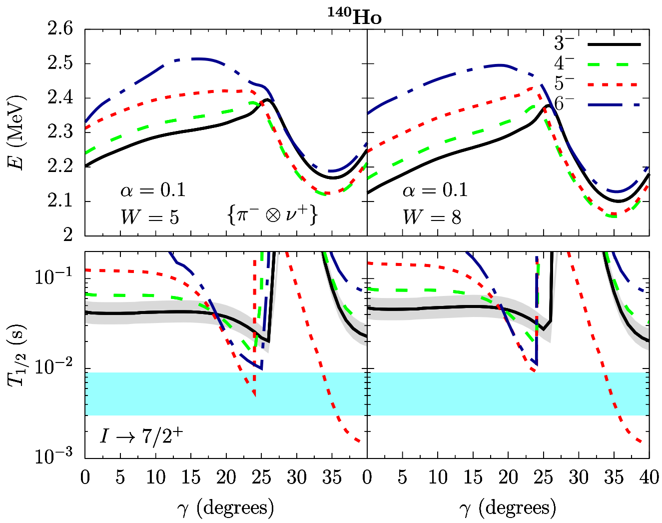

FIG. 6. Same as Fig. 5 but with zero-range *np* interaction.

while identifying the possible candidates for the ground state. Since the lowest lying state is 3^- for both forms of *np* interaction, this can be considered as the most favored candidate for the ground state from which the proton emission occurs.

We proceed to investigate the role of *np* interaction on the other possible channel, i.e., proton emission to $9/2^-$ state of the daughter nucleus. The results obtained with the constant potential form are given in Fig. 7. In the presence of GM splitting, the 8^+ turns out to be the lowest lying state, lifting its degeneracy with 3^+. Unlike the case of negative parity states, the effect of Newby shift is negligible. Similarly to the case of negative parity states, the half-lives are almost insensitive to the *np* interaction. The half-life corresponding to the 8^+ state is still far from the measured value. We obtained similar conclusions from the zero-range interaction (not shown here). Therefore, the proton emission to the $9/2^-$ state is very unlikely.

To further support the above arguments, we proceed to calculate the branching ratios to possible first excited states of the daughter, i.e., $5/2^+$ and $11/2^-$, and the results are given in Fig. 8. At very low γ, the $5/2^+$ state is the lowest in energy, and hence 100% of the decay proceeds to this state. However, the corresponding half-lives are far from the measured values, so we discard this possible decay channel. The calculated branching ratios to $5/2^+$ state of the daughter are insignificant for all considered states in the region with $20^\circ \lesssim \gamma \lesssim 25^\circ$. Outside this γ region, the branching ratio for 6^- state is very large. Since the half-lives agree with the measured data in the $20^\circ \lesssim \gamma \lesssim 25^\circ$ region only, the calculated branching ratios outside this region are not meaningful. These observations again support the deformation being close to that of ^{141}Ho [12]. In the case of proton emission populating the $11/2^-$ state of the daughter, the branching ratio is quite significant except for the emission from the 3^+ and 8^+ states. The measurements do not suggest any branching and hence none of these states can be the proton emitting one. The branching ratios for the 3^+

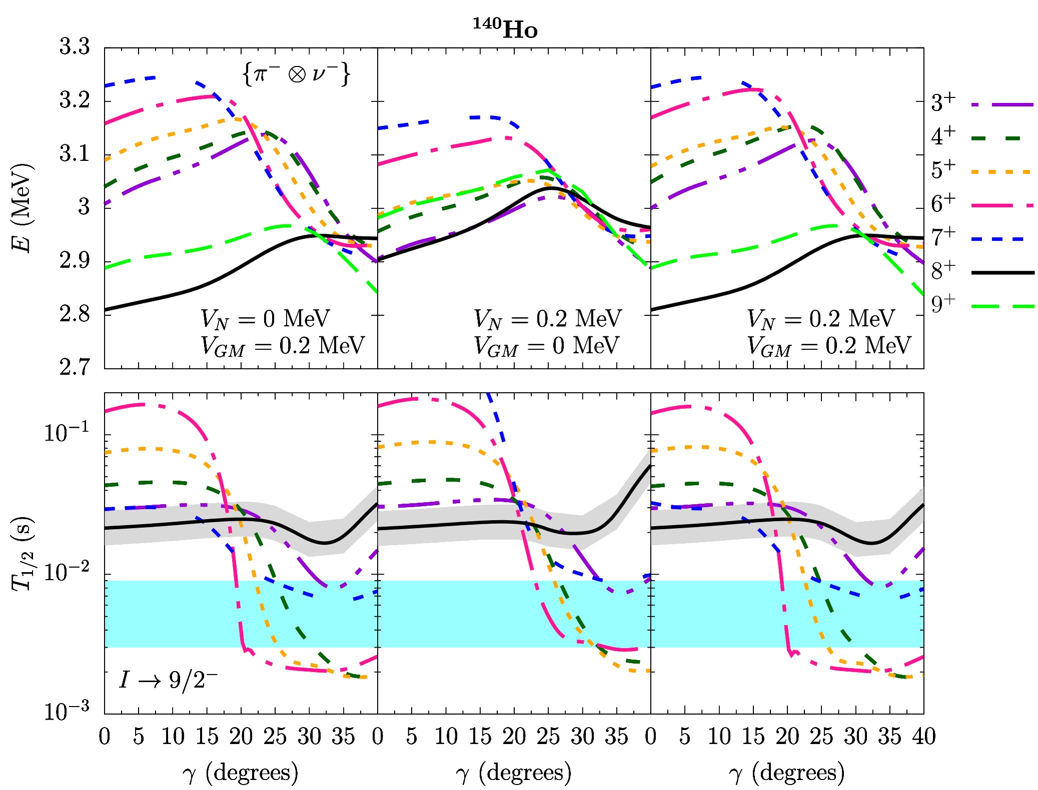

FIG. 7. Rotational energies (top panels) and the proton emission half-lives (bottom panels) from positive parity states of ^{140}Ho to the $9/2^-$ state of the daughter for different sets of parameters of constant potential *np* interaction.

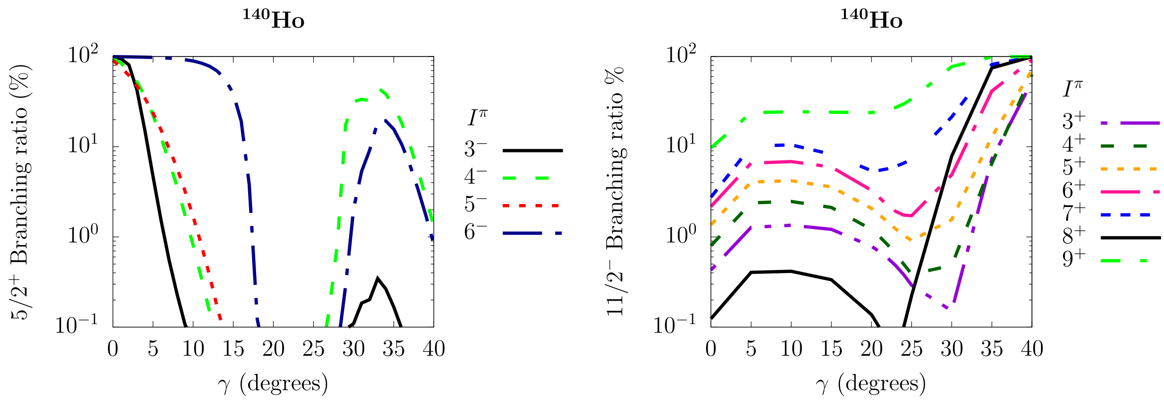

FIG. 8. The branching ratios for proton emission from the negative parity states of ^{140}Ho to the $5/2^+$ (left) state of ^{139}Dy (daughter) and from the positive parity states of ^{140}Ho to the $11/2^-$ (right) state of ^{139}Dy (daughter).

and 8^+ states are quite low in the probable deformation region but the corresponding half-lives are far from the experimental data. Hence, any decay to the negative parity state of the daughter can be ruled out. These observations allow us to unambiguously assign the ground state of the daughter nucleus with the spin and parity $7/2^+$. This assignment is in agreement with the one suggested in a study based on β-delayed proton measurement [16]. Therefore, 3^- is the proton emitting state in ^{140}Ho.

The contribution of single-particle configurations given in Fig. 9 reveals that the dominant configuration for 3^- is $\{\pi h^{4th}_{11/2} \otimes \nu g^{4th}_{7/2}\}$ with significant contributions from $\{\pi h^{3rd}_{11/2} \otimes \nu g^{4th}_{7/2}\}$ and $\{\pi h^{5th}_{11/2} \otimes \nu g^{4th}_{7/2}\}$. With increase in spin, the contribution of $\{\pi h^{3rd}_{11/2} \otimes \nu g^{4th}_{7/2}\}$ increases and becomes equally dominant as $\{\pi h^{4th}_{11/2} \otimes \nu g^{4th}_{7/2}\}$ at 6^-. The plot of $p(|K|)$, the probability distribution of $K[=K_R + (\Omega_p \pm \Omega_n)]$ is also shown in Fig. 9. In the case of 3^-, we observe the dominance of $K = 0$ with probability more than 50%, followed by $K = 1$. This probability is almost equal for $K = 0$ and $K = 1$ in the case of 4^-. For the states 5^- and 6^-, the distribution flattens over a broad range of K. From the asymptotic quantum numbers and noticing that K_R (projection of R on the 3 axis) is close to zero for lower lying states, one can see whether a state is predominantly a triplet or a singlet. For example, the asymptotic quantum numbers [17] for the single-particle states $\pi h^{4th}_{11/2}$ and $\nu g^{4th}_{7/2}$ are [523]7/2 and [404]7/2, respectively. In the case of 3^-, we get $K = 0$ from $\Omega_p - \Omega_n$ which gives total intrinsic spin projection $\Sigma = 1$. Hence, 3^- is predominantly a triplet state and is consequently favored by the GM splitting. The dominance of $K = 0$ further explains large Newby shift in 3^- due to the odd spin as shown in Fig. 5.

Similarly to Fig. 9, the contribution of single-particle configurations and $p(|K|)$ corresponding to the positive parity states are given in Fig. 10. In case of $3^+, 4^+$, and 8^+, the single-particle configuration $\{\pi h^{4th}_{11/2} \otimes \nu h^{5th}_{11/2}\}$ is the dominant one. At the intermediate spins, the configuration $\{\pi h^{3rd}_{11/2} \otimes \nu h^{5th}_{11/2}\}$ becomes equally dominant as $\{\pi h^{4th}_{11/2} \otimes \nu h^{5th}_{11/2}\}$. The asymptotic quantum numbers for the single-particle states $\pi h^{4th}_{11/2}$ and $\nu h^{5th}_{11/2}$ are [523]7/2 and [514]9/2, respectively. The $p(|K|)$ corresponding to the 8^+ state is maximum for $K = 8$ with a probability of nearly 60%. The

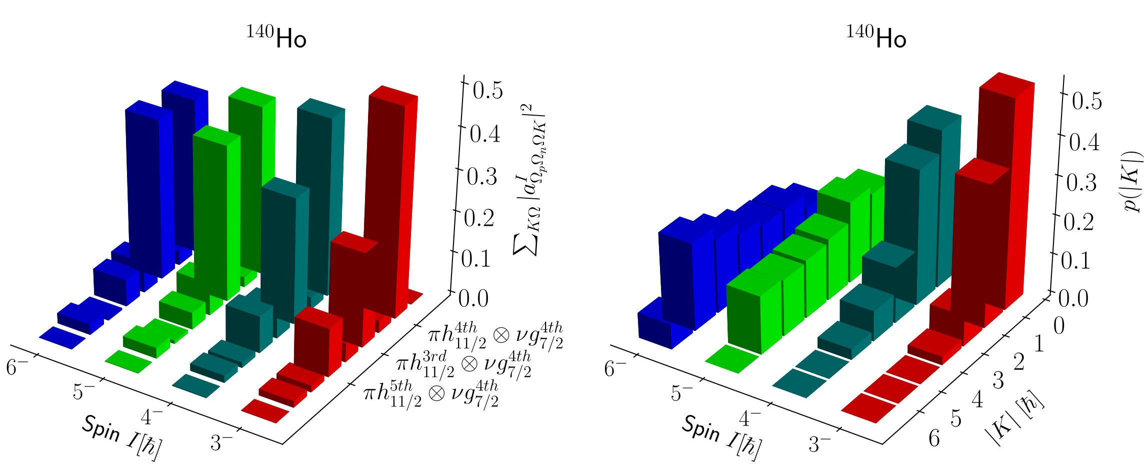

FIG. 9. Contribution of various single-particle configurations (left) and probability distribution of K (right) in negative parity rotational states of ^{140}Ho at $\gamma = 24^\circ$.

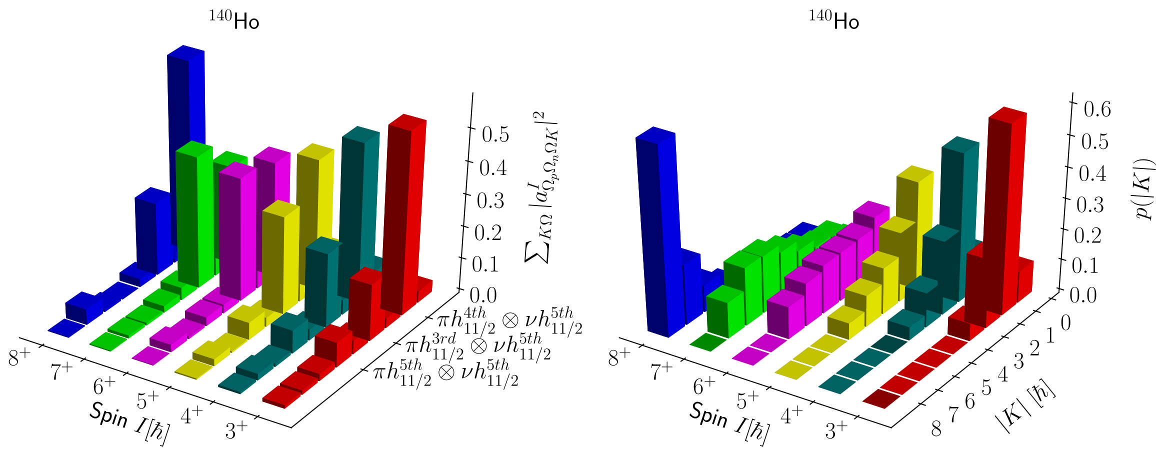

FIG. 10. Same as Fig. 9 but for positive parity states.

$K = 8$ originates from $\Omega_p + \Omega_n$ with $\Sigma = 1$. Hence, the 8^+ is predominantly a triplet state and is favored by the GM splitting. Since the probability for $K = 0$ is nearly 0%, the Newby shift is almost negligible, as noticed from results with *np* interaction shown in Fig. 7. In case of 3^+, the $p(|K = 1|)$ is dominant, suggesting it to be a singlet state, which is not favored by the GM splitting.

The proton emission decay width [Eq. (3)] is a result of interplay between several quantities, which can vary independently of each other. Among these quantities, the mixing coefficients a of the parent wave function are useful to understand the correlation between decay width and the residual *np* interaction. With the introduction of residual *np* interaction, if a dominant single-particle configuration sustains its dominance, the values of a do not change significantly. A significant change in the configuration leads to a strong variation in a's, and hence affects the half-life. For example, at $\gamma \approx 24^\circ$, the single-particle configurations shown in Figs. 9 and 10 are similar after including *np* interaction (not shown here) except for a slight increase in the dominance of $\{\pi h^{4th}_{11/2} \otimes \nu g^{4th}_{7/2}\}$. However, at $\gamma = 0^\circ$, in the cases of $3^-, 4^-$, and 5^- the dominant configuration $\{\pi h^{4th}_{11/2} \otimes \nu g^{3rd}_{7/2}\}$ changes to $\{\pi h^{4th}_{11/2} \otimes \nu g^{4th}_{7/2}\}$ (due to larger overlap of proton and neutron wave functions) with the inclusion of *np* interaction. The configuration for 6^- is not affected by *np* interaction. Therefore, the half-lives are sensitive to the residual *np* interaction at $\gamma = 0^\circ$, but not at higher γ.

IV. CONCLUSIONS

The proton emission from ^{140}Ho is studied in detail within the nonadiabatic quasiparticle approach considering the role of residual neutron-proton interaction and triaxiality. We assign the ground state spin and parity of the daughter (^{139}Dy) to be $7/2^+$. The triaxial deformation is found to be very crucial in explaining the measured data with its value $\gamma \approx 25^\circ$. The proton emitting state of ^{140}Ho is assigned as 3^- which is predominantly a triplet state with the configuration $\{\pi h^{4th}_{11/2} \otimes \nu g^{4th}_{7/2}\}$. The effect of the residual *np* interaction is investigated and found to be helpful in assigning the ground state. The calculated branching ratios further eradicate many ambiguities in assigning the ground state spin and parity for both ^{139}Dy and ^{140}Ho.

ACKNOWLEDGMENT

This work was supported in part by the U.S. Department of Energy, Office of Science, Office of High Energy Physics, under Award No. DE-SC0019465.

[1] B. Blank and M. J. G. Borge, Prog. Part. Nucl. Phys. **60**, 403 (2008).
[2] H. Suzuki, L. Sinclair, P.-A. Söderström, G. Lorusso, P. Davies, L. S. Ferreira, E. Maglione, R. Wadsworth, J. Wu, Z. Y. Xu *et al.*, Phys. Rev. Lett. **119**, 192503 (2017).
[3] K. Auranen, D. Seweryniak, M. Albers, A. Ayangeakaa, S. Bottoni, M. Carpenter, C. Chiara, P. Copp, H. David, D. Doherty *et al.*, Phys. Lett. B **792**, 187 (2019).
[4] D. T. Doherty, A. N. Andreyev, D. Seweryniak, P. J. Woods, M. P. Carpenter, K. Auranen, A. D. Ayangeakaa, B. B. Back, S. Bottoni, L. Canete *et al.*, Phys. Rev. Lett. **127**, 202501 (2021).
[5] K. Auranen, A. D. Briscoe, L. S. Ferreira, T. Grahn, P. T. Greenlees, A. Herzáň, A. Illana, D. T. Joss, H. Joukainen, R. Julin *et al.*, Phys. Rev. Lett. **128**, 112501 (2022).
[6] T. Kubo, D. Kameda, H. Suzuki, N. Fukuda, H. Takeda, Y. Yanagisawa, M. Ohtake, K. Kusaka, K. Yoshida, N. Inabe *et al.*, Prog. Theor. Exp. Phys. **2012**, 03C003 (2012).
[7] P. Möller, A. J. Sierk, T. Ichikawa, and H. Sagawa, At. Data Nucl. Data Tables **109-110**, 1 (2016).
[8] D. M. Cullen, M. P. Carpenter, C. N. Davids, A. M. Fletcher, S. J. Freeman, R. V. F. Janssens, F. G. Kondev, C. J. Lister, L. K. Pattison, D. Seweryniak *et al.*, Phys. Lett. B **529**, 42 (2002).
[9] F. R. Xu, P. M. Walker, and R. Wyss, Phys. Rev. C **59**, 731 (1999).

[10] K. Rykaczewski, J. C. Batchelder, C. R. Bingham, T. Davinson, T. N. Ginter, C. J. Gross, R. Grzywacz, M. Karny, B. D. MacDonald, J. F. Mas *et al.*, Phys. Rev. C **60**, 011301(R) (1999).
[11] L. S. Ferreira and E. Maglione, Phys. Rev. Lett. **86**, 1721 (2001).
[12] P. Arumugam, L. Ferreira, and E. Maglione, Phys. Lett. B **680**, 443 (2009).
[13] P. Siwach, P. Arumugam, S. Modi, L. S. Ferreira, and E. Maglione, J. Phys. G: Nucl. Part. Phys. **47**, 125105 (2020).
[14] P. Siwach, P. Arumugam, S. Modi, L. S. Ferreira, and E. Maglione, Phys. Rev. C **103**, L031303 (2021).
[15] P. Siwach, P. Arumugam, S. Modi, L. S. Ferreira, and E. Maglione, Phys. Rev. C **105**, L031302 (2022).
[16] S.-W. Xu, Z.-K. Li, Y.-X. Xie, Q.-Y. Pan, Y. Yu, J. Adam, C.-F. Wang, J.-P. Xing, Q.-Y. Hu, S.-H. Li *et al.*, Phys. Rev. C **60**, 061302(R) (1999).
[17] A. Bohr and B. R. Mottelson, *Nuclear Structure* (Benjamin, New York, 1969), Vol. II.